Mon. Not. R. Astron. Soc. **392,** 1585–1590 (2009) doi:10.1111/j.1365-2966.2008.14164.x

WASP-10b: a 3M_J, gas-giant planet transiting a late-type K star

D. J. Christian,[1,2⋆] N. P. Gibson,[1] E. K. Simpson,[1] R. A. Street,[1,3] I. Skillen,[4] D. Pollacco,[1] A. Collier Cameron,[5] Y. C. Joshi,[1] F. P. Keenan,[1] H. C. Stempels,[5] C. A. Haswell,[6] K. Horne,[5] D. R. Anderson,[7] S. Bentley,[7] F. Bouchy,[8,9] W. I. Clarkson,[6,10] B. Enoch,[6] L. Hebb,[5] G. Hébrard,[8] C. Hellier,[7] J. Irwin,[11] S. R. Kane,[12] T. A. Lister,[3,5,7] B. Loeillet,[13] P. Maxted,[7] M. Mayor,[14] I. McDonald,[7] C. Moutou,[13] A. J. Norton,[6] N. Parley,[6] F. Pont,[14,15] D. Queloz,[14] R. Ryans,[1] B. Smalley,[7] A. M. S. Smith,[5] I. Todd,[1] S. Udry,[14] R. G. West,[16] P. J. Wheatley[17] and D. M. Wilson[7]

[1]*Astrophysics Research Centre, School of Mathematics and Physics, Queen's University, University Road, Belfast, BT7 1NN*
[2]*Department of Physics and Astronomy, California State University Northridge, 18111 Nordhoff Street, Northridge, CA 91330-8268, USA*
[3]*Las Cumbres Observatory, 6740 Cortona Dr Suite 102, Santa Barbara, CA 93117, USA*
[4]*Isaac Newton Group of Telescopes, Apartado de Correos 321, E-38700 Santa Cruz de la Palma, Tenerife, Spain*
[5]*School of Physics and Astronomy, University of St Andrews, North Haugh, St Andrews, Fife KY16 9SS*
[6]*Department of Physics and Astronomy, The Open University, Milton Keynes, MK7 6AA*
[7]*Astrophysics Group, Keele University, Staffordshire, ST5 5BG*
[8]*Institut d'Astrophysique de Paris, CNRS (UMR 7095) – Université Pierre and Marie Curie, 98bis bvd. Arago, 75014 Paris, France*
[9]*Observatoire de Haute-Provence, 04870 St Michel l'Observatoire, France*
[10]*STScI, 3700 San Martin Drive, Baltimore, MD 21218, USA*
[11]*Harvard–Smithsonian Center for Astrophysics, 60 Garden Street, Cambridge, MA 02138, USA*
[12]*Michelson Science Center, Caltech, MS 100-22, 770 South Wilson Avenue Pasadena, CA 91125, USA*
[13]*Laboratoire d'Astrophysique de Marseille, BP 8, 13376 Marseille Cedex 12, France*
[14]*Observatoire de Genève, Université de Genève, 51 Ch. des Maillettes, 1290 Sauverny, Switzerland*
[15]*School of Physics, University of Exeter, Stocker Road, Exeter, EX4 4QL*
[16]*Department of Physics and Astronomy, University of Leicester, Leicester, LE1 7RH*
[17]*Department of Physics, University of Warwick, Coventry, CV4 7AL*

Accepted 2008 October 29. Received 2008 October 28; in original form 2008 September 10

ABSTRACT

We report the discovery of WASP-10b, a new transiting extrasolar planet (ESP) discovered by the Wide Angle Search for Planets (WASP) Consortium and confirmed using Nordic Optical Telescope FIbre-fed Echelle Spectrograph and SOPHIE radial velocity data. A 3.09-d period, 29 mmag transit depth and 2.36 h duration are derived for WASP-10b using WASP and high-precision photometric observations. Simultaneous fitting to the photometric and radial velocity data using a Markov Chain Monte Carlo procedure leads to a planet radius of 1.28R_J, a mass of 2.96M_J and eccentricity of ≈0.06. WASP-10b is one of the more massive transiting ESPs, and we compare its characteristics to the current sample of transiting ESP, where there is currently little information for masses greater than ≈2M_J and non-zero eccentricities. WASP-10's host star, GSC 2752−00114 (USNO-B1.0 1214−0586164) is among the fainter stars in the WASP sample, with $V = 12.7$ and a spectral type of K5. This result shows promise for future late-type dwarf star surveys.

Key words: methods: data analysis – techniques: photometric – techniques: radial velocities – stars: planetary systems.

1 INTRODUCTION

Photometric transit observations of extrasolar planets (ESP) are important because the transit strongly constrains their orbital inclination and allows accurate physical parameters for the planet to be

⋆E-mail: d.christian@qub.ac.uk

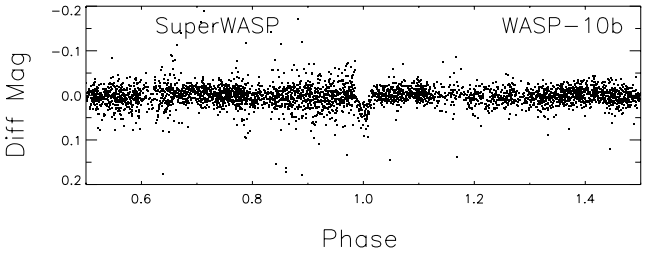

Figure 1. Shown is the un-binned SuperWASP folded light curve for WASP-100b (1SWASP J231558.30+312746.4). The data were phased using the ephemeris, $T_O = 2454357.85808^{+0.00041}_{-0.00036}$ $P = 3.09276$ d.

derived. Their mass–radius relation allows us to probe their internal structure and is vital to our understanding of orbital migration and planetary formation. The radial velocity (RV) measurements which are used to confirm a candidate transiting ESP also provide more complete information on the orbital eccentricity.

As wide-field photometric transit surveys have collected additional sky and temporal coverage, and understood their noise components (Collier Cameron et al. 2007a; Smith et al. 2007), the number of transiting ESP has grown to over 50 in line with earlier predictions (Horne 2003). Recently, one such survey SuperWASP (Pollacco et al. 2006) published its first five confirmed ESP, all of which have periods of less than 3 d (Anderson et al. 2008; Collier Cameron et al. 2007b; Pollacco et al. 2008; Wilson et al. 2008), and reported an additional 10[1] (Hellier et al. 2008; Hebb et al. 2008; Joshi et al. 2008; West et al. 2008). SuperWASP is performing a 'shallow-but-wide' transit search, designed to find planets that are not only sufficiently bright ($9 < V < 13$) for high-precision RV follow-up to be feasible on telescopes of moderate aperture, but also for detailed studies such as transmission spectroscopy during transits. Details of the WASP project and observatory infrastructure are described in Pollacco et al. (2006).

In this paper, we present the WASP photometry of 1SWASP J231558.30+312746.4 (GSC 2752−00114), higher precision photometric follow-up observations with the MERCATOR and Tenagra telescopes and high-precision RV observations with the Nordic Optical Telescope new FIbre-fed Echelle Spectrograph (FIES) and the Observatoire de Haute-Provence (OHP) SOPHIE collaboration. These observations lead to the discovery and confirmation of a new, relatively high-mass, gas-giant exoplanet, WASP-10b.

2 OBSERVATIONS

1SWASP J231558.30+312746.4 (GSC 2752−00114) was monitored by SuperWASP-N starting in 2004. SuperWASP is a multi-camera telescope system with SuperWASP-North located in La Palma and consisting of 8 Canon 200-mm f/1.8 lenses each coupled to e2v 2048 × 2048 pixel back illuminated CCDs. This combination of lens and camera yields a field of view of 7.°8 × 7.°8 with an angular size of 14.2 arcsec per pixel. During 2004, SuperWASP was run with four or five cameras as the operations moved from commissioning to routine automated observing. We show the WASP-10b SuperWASP light curve in Fig. 1.

2.1 Higher precision photometry

We obtained photometry of WASP-10 with the MEROPE instrument on the 1.2 m MERCATOR Telescope in V band on 2007 September 1. Only a partial transit was observed due to uncertainties in the period and epoch from the SuperWASP data. Observations were in the V band with 2 × 2 binning over ∼2.9 h. Despite clear conditions, exposure times were varied from 25 to 30 s to account for changes in seeing and to keep below the saturation limits of the chip. This allowed 170 images to be taken. There was a drift of only 1 binned pixel in x and y on the chip during the run. The MEROPE images were first de-biased and flat-fielded with combined twilight flats using IRAF and the APPHOT package to obtain aperture photometry of the target and five nearby companion stars using a 10 pixel radius. Finally, the light curve was extracted and normalized to reveal a depth of ∼33 mmag.

Further observations of WASP-10 were taken as part of an observing program sponsored by the Las Cumbres Observatory Global Telescope Network[2] on the Tenagra II, 0.81 m F7 Ritchey–Chretien telescope sited in the Sonora desert in S. Arizona, USA. The science camera contains a 1 × 1 k SITe CCD with a pixel scale of 0.87 arcsec pixel^{-1} and a field of view of 14.8 × 14.8 arcmin^2. The filter set is the standard Johnson/Cousins/Bessel *UBVRI* set and the data presented here have been taken in I band.

Calibration frames were obtained automatically every twilight, and the data were de-biased and flat-fielded using the calibration section of the SuperWASP pipeline. Object detection and aperture photometry were then performed using DAOPHOT (Stetson 1987) within IRAF. Differential photometry was derived from a selection of typically 5 to 10 comparison stars within the frame.

These confirmed that the object had a sharp egress with an amplitude of 0.033 ± 0.001 mag. The MERCATOR V and Tenagra I light curves show consistent transit depths, confirming that the companion is a transiting ESP.

2.2 Spectroscopic follow-up

We obtained high-precision RV follow-up observations of WASP-10 with the 2.5 m Nordic Optical Telescope (NOT) new FIES, supplemented with observations from the Observatoire de Haute–Provence's 1.93 m telescope and the SOPHIE spectrograph (Bouchy et al. 2006). We present a summary of the FIES and SOPHIE RV data in Table 1.

2.2.1 NOT and FIES

Spectroscopic observations were obtained using the new FIES spectrograph mounted on the NOT Telescope. A total of seven RV points were obtained during 2007 December 2, 28–31 and 2008 January 24–25. WASP-10 required observations with an exposure time of 2400 s due its relative faintness ($V = 12.7$) yielding a peak signal-to-noise ratio per resolution element of ≈60–70 in the Hα region. FIES was used in medium resolution mode with $R = 46\,000$ with simultaneous ThAr calibration. We used the bespoke data reduction package FIESTOOL[3] to extract the spectra and a specially developed IDL line-fitting code to obtain RVs with a precision of 15–25 m s^{-1} (except for the poor night of 2008 January 24, JD 2454490).

2.2.2 OHP 1.9 m and SOPHIE

Additional RV measurements were taken for WASP-10 on 29 and 30 August 2007, and again between 2008 Feb 11 and 15 with

[1] http://www.inscience.ch/transits/

[2] www.lcogt.net

[3] http://www.not.iac.es/instruments/fies/fiestool/FIEStool.html

Table 1. Journal of RV measurements for WASP-10 (1SWASP J231558.30+312746.4, USNO-B1.0 1214−0586164). Stellar coordinates are for the photometric apertures; the USNO-B1.0 number denotes the star for which the RV measurements were secured. The quoted uncertainties in the RV errors include components due to photon noise (Section 2.2) and 10 m s^{-1} of jitter (Section 3.2) added in quadrature.

BJD	$t_{\rm exp}$ (s)	$V_{\rm r}$ km s^{-1}
FIES		
2454437.540	2400	-11.028 ± 0.026
2454463.377	2400	-11.941 ± 0.030
2454465.342	2400	-11.003 ± 0.018
2454466.335	2400	-11.804 ± 0.021
2454490.329	2400	-11.013 ± 0.143
2454490.358	2400	-10.990 ± 0.120
2454491.340	2400	-11.955 ± 0.024
SOPHIE		
2454340.569	3300	-11.657 ± 0.008
2454342.505	3600	-11.575 ± 0.011
2454508.262	1680	-11.027 ± 0.014
2454509.268	1680	-11.336 ± 0.017
2454510.276	1680	-11.990 ± 0.020
2454511.262	1680	-11.135 ± 0.016
2454512.262	1680	-11.244 ± 0.016

the OHP 1.93 m telescope and the SOPHIE spectrograph (Bouchy et al. 2006), a total of seven usable spectra were acquired. We used SOPHIE in its high-efficiency mode, acquiring simultaneous star and sky spectra through separate fibers with a resolution of $R = 40\,000$. Thorium–Argon calibration images were taken at the start and end of each night, and at 2- to 3-h intervals throughout the night. The RV drift never exceeded 2 to 3 m s^{-1}, even on a night-to-night basis. Although errors for each RV measurement are limited by the photon noise. Thus, the average RV error is ≈14 m s^{-1} and includes the 2 to 3 m s^{-1} systematic error and the contribution from the photon noise. Typical signal-to-noise ratio estimates for each spectra were ≈30 (near 5500 Å). The SOPHIE WASP-10 spectra were cross-correlated against a K5V template provided by the SOPHIE control and reduction software. Typical full width at half-maximum (FWHM) and contrasts for these spectra were ≈10.2–10.4 km s^{-1} and 30–31 per cent, respectively. The cross-correlation techniques and derivation of errors in the RV measurements are presented in Pollacco et al. (2008).

3 RESULTS AND ANALYSIS

3.1 Stellar parameters

We merged all available WASP-10 FIES spectra into one high-quality spectrum in order to perform a detailed spectroscopic analysis of the stellar atmospheric properties. Radial velocity signatures were carefully removed during the process. This merged spectrum was then continuum normalized with a low-order polynomial to retain the shape of the broadest spectral features. The total signal-to-noise ratio of the combined spectrum was ≈180 per pixel. We were not able to include the SOPHIE spectra in this analysis, because these spectra were obtained in the high-efficiency (HE) mode, which is known to suffer from problems with removal of the blaze function.

Table 2. Stellar parameters for WASP-10. The last five parameters were derived from the SME analysis of the FIES spectroscopy.

Parameter	WASP-10
RA (J2000)	23 15 58.3
Dec. (J2000)	+31 27 46.4
V	12.7
Distance	90 ± 20 pc
$T_{\rm eff}$	4675 ± 100 K
log g	4.40 ± 0.20
[M/H]	0.03 ± 0.20
$v \sin i$	<6 km s^{-1}
$v_{\rm rad}$	-11.44 ± 0.03 km s^{-1}

As previously undertaken for our analysis of WASP-1 (Stempels et al. 2007) and WASP-3 (Pollacco et al. 2008), we employed the methodology of Valenti & Fischer (2005), using the same tools, techniques and model atmosphere grid. We used the package *Spectroscopy Made Easy* (SME) (Valenti & Piskunov 1996), which combines spectral synthesis with multidimensional χ^2 minimization to determine which atmospheric parameters best reproduce the observed spectrum of WASP-10 (effective temperature $T_{\rm eff}$, surface gravity log g, metallicity [M/H], projected RV $v \sin i$, systemic RV $v_{\rm rad}$, microturbulence $v_{\rm mic}$ and the macroturbulence $v_{\rm mac}$).

The four spectral regions we used in our analysis are: (i) 5160–5190 Å, covering the gravity-sensitive Mg b triplet; (ii) 5850–5950 Å, with the temperature and gravity-sensitive Na I D doublet; (iii) 6000–6210 Å, containing a wealth of different metal lines, providing leverage on the metallicity, and (iv) 6520–6600 Å, covering the strongly temperature-sensitive Hα line. In addition, we analysed a small region around the Li I 6708 line to possibly derive a lithium abundance, but no Li I 6708 was detected for WASP-10. The parameters we obtained from this analysis are listed in Table 2. In addition to the spectral analysis, we also use available photometry [from The Amateur Sky Survey (NOMAD), Naval Observatory Merged Astrometric Dataset (TASS4) and Carlsberg Meridian Catalogue 14 (CMC14) catalogues] plus Two-Micron All-Sky Survey to estimate the effective temperature using the infrared flux method (Blackwell & Shallis 1977). This yields $T_{\rm eff} = 4650 \pm 120$ K, which is in agreement with the spectroscopic analysis and a spectral type of K5. The characteristics of WASP-10 are also given in Table 2.

3.2 Markov Chain Monte Carlo analysis

Transit timing and the RV measurements provide detailed information about the orbit. We modelled WASP-10b's transit photometry and the reflex motion of the host star simultaneously using the Markov Chain Monte Carlo (MCMC) algorithm described in detail by Collier Cameron et al. (2007a), and the same techniques that were applied to WASP-3 by Pollacco et al. (2008) to which we refer the reader for more details.

We find WASP-10b to have a radius $1.28^{+0.08}_{-0.09} R_J$, mass of $2.96^{+0.22}_{-0.17}$ M_J and a significant non-zero eccentricity of $0.059^{+0.014}_{-0.004}$. The best-fitting solution for the MCMC model for a circular orbit ($e = 0$) has a χ^2 55 higher than the solution with a non-zero eccentricity, and thus, the eccentricity is significant at >99.6 per cent confidence level using the F test. The values of the parameters of the optimal solution are given, together with their associated 1σ confidence intervals, in Table 3. The FIES + SOPHIE RV data measurements are plotted in Fig. 2 together with the best-fitting global fit to the SuperWASP-N, MERCATOR and Tenagra transit photometry.

Table 3. WASP-10 system parameters and 1σ error limits derived from MCMC analysis.

Parameter	Symbol	Value
Transit epoch (BJD)	T_0	$2454357.85808^{+0.00041}_{-0.00036}$ d
Orbital period	P	$3.0927636^{+0.0000094}_{-0.000021}$ d
Planet/star area ratio	$(R_p/R_s)^2$	$0.029^{+0.001}_{-0.001}$
Transit duration	t_T	$0.098181^{+0.0019}_{-0.0015}$ d
Impact parameter	b	$0.568^{+0.054}_{-0.084}$ R_*
Stellar reflex velocity	K_1	$0.5201^{+0.0084}_{-0.010}$ km s^{-1}
Centre-of-mass velocity	γ	$-11.4854^{+0.0012}_{-0.0034}$ km s^{-1}
Orbital semimajor axis	a	$0.0369^{+0.0012}_{-0.0014}$ AU
Orbital inclination	I	$86.9^{+0.6}_{-0.5}$ degrees
Orbital eccentricity	ϵ	$0.059^{+0.014}_{-0.004}$
Arg. periastron	ω	$2.917^{+0.222}_{-0.245}$ (rad)
Stellar mass	M_*	$0.703^{+0.068}_{-0.080}$ M$_\odot$
Stellar radius	R_*	$0.775^{+0.043}_{-0.040}$ R$_\odot$
Stellar surface gravity	$\log g_*$	$4.51^{+0.06}_{-0.05}$ (CGS)
Stellar density	ρ_*	$1.51^{+0.25}_{-0.20}$ $\rho_\odot$
Planet radius	R_p	$1.28^{+0.077}_{-0.091}$ R_J
Planet mass	M_p	$2.96^{+0.22}_{-0.17}$ M_J
Planetary surface gravity	$\log g_p$	3.62 ± 0.06 (CGS)
Planet density	ρ_p	$1.43^{+0.31}_{-0.29}$ ρ_J
Planet temp ($A = 0$)	T_{eql}	1119^{+26}_{-28} K
χ^2_ν (photometric)	χ^2_{phot}	4145
Photometric data points	N_{phot}	4151
χ^2_ν (spectroscopic)	χ^2_{spec}	17.2
Spectroscopic data points	N_{spec}	14

3.3 Line-bisector variation

Line bisectors have been shown to be a powerful diagnostic in distinguishing true ESPs from blended and eclipsing stellar systems chromospheric activity (Queloz et al. 2001). Torres et al. (2004) showed that for OGLE-TR-33 line asymmetries which changed with a 1.95-d period, it was a blended system. From the cross-correlation function (CCF), we obtained the line bisectors and these are plotted, as a function of RV, in Fig. 3.

We quantified the significance of the bisector variation as follows. We determined the inverse-variance-weighted averages of the RV and bisector span as

$$\hat{v} = \frac{\sum_i v_i w_i}{\sum_i w_i}; \hat{b} = \frac{\sum_i b_i w_i}{\sum_i w_i},$$

where the v_i and b_i are the RV and span bisector values, respectively, and the weights w_i are the inverse variances of the individual bisector measurements. The uncertainty in the span bisector is assumed to be 2.5 times the uncertainty on the RV in our data. If we define $x_i = v_i - \hat{v}$ and $y_i = b_i - \hat{b}$, then the slope is determined as

$$\hat{a} = \frac{\sum_i x_i y_i w_i}{\sum_i x_i^2 w_i}; \mathrm{Var}(\hat{a}) = \frac{1}{\sum_i x_i^2 w_i}.$$

The value of the scaling factor $\hat{a}$ is determined with a signal-to-noise ratio

$$\mathrm{SNR} = \frac{\hat{a}}{\sqrt{Var(\hat{a})}}.$$

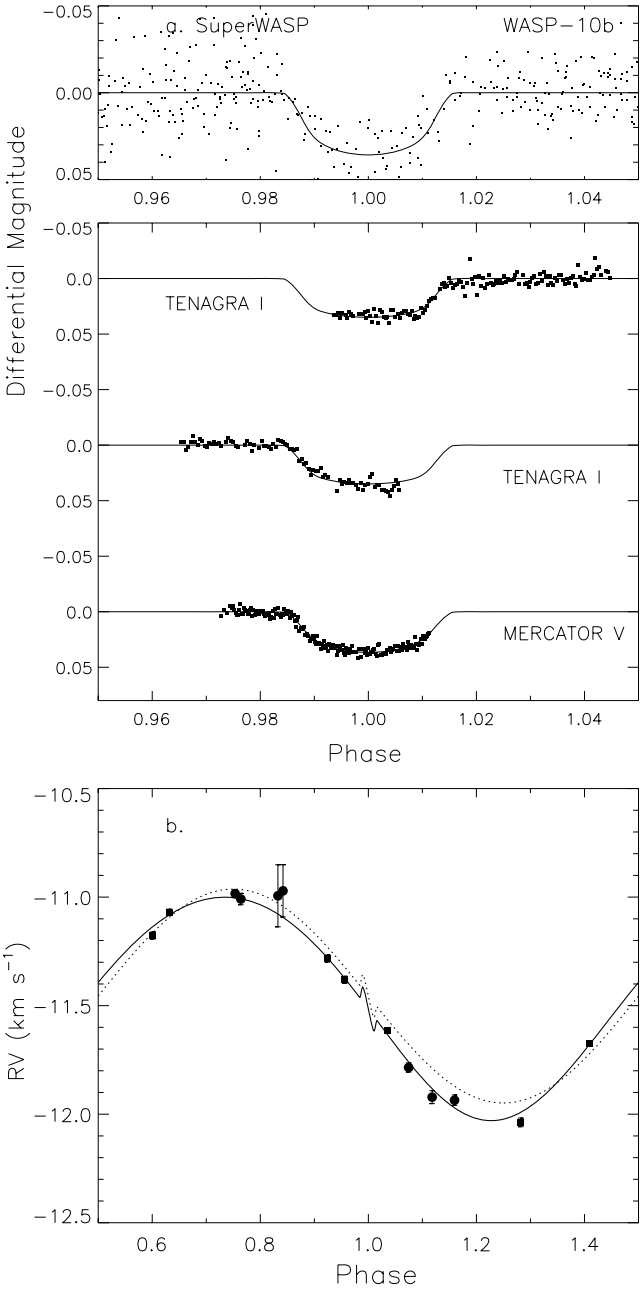

Figure 2. Simultaneous MCMC solutions to the WASP-10 photometry and RV data. (a) The top panels show the MCMC solutions to the combined SuperWASP-N, MERCATOR V and Tenagra I band photometry. All the data (apart from that from SuperWASP-N) were averaged in 300s bins). (b) The lower panel shows the MCMC solution to the FIES + SOPHIE RV data. (FIES RVs are shown as filled circles and SOPHIE as filled squares). The model fit to the RV data includes orbital eccentricity (solid line), and for a circular orbit (dashed line). Both RV models also include the Rossiter–McLaughlin effect, which is small for this system given the low $v \sin i$ of the host star (<6 km s^{-1}).

We obtain SNR = 1.16 indicating a non-significant correlation between the bisector span and RV variations. This demonstrates that the CCF remains symmetric, and that the RV variations are not likely to be caused by line-of-site binarity or stellar activity and indicate WASP-10b is an exoplanet.

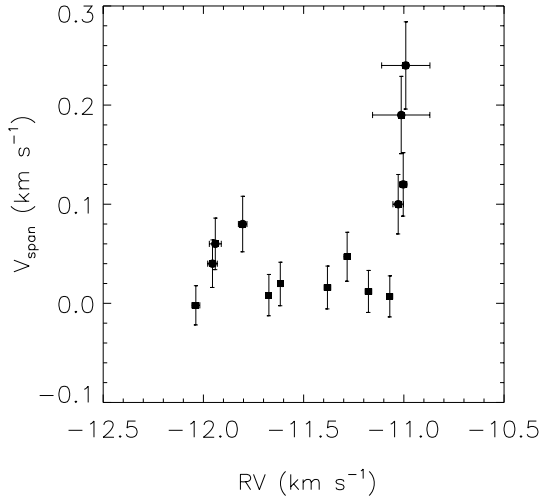

Figure 3. Line bisectors as a function of RV for WASP-10. Plot symbols are the same as Fig. 2. Analysis of these line bisectors for WASP-10 does not show a correlation between the bisector velocity ($V_{\rm span}$) and stellar RV (see the text).

4 DISCUSSION

Photometric surveys have now provided a large sample of transiting ESP that can be used to determine their mass–radius relation and provide constraints on their compositions. Here, we presented the discovery of a new ESP with a mass of $2.96 M_J$, $1.28 R_J$ radius and a significant eccentricity of $0.059^{+0.014}_{-0.004}$. We now discuss the properties of WASP-10b in relation to the current sample of transiting ESP, starting with its non-zero eccentricity.

Most of the current sample of published transiting ESP have orbits consistent with being circular and are fit with models using zero eccentricity as is expected for short-period planets in orbits with semimajor axes <0.2 au. Recent work (Jackson, Greenberg & Barnes 2008; Mardling 2007, and references therein) has investigated the effects of tidal dissipation on the orbits of short-period ESP. The evolution of the orbital eccentricity appears to be driven primarily by tidal dissipation within the planet, giving a circularization time-scale substantially less than 1 Gyr for typical tidal dissipation parameter, $Q_{\rm p} = 10^5$ to 10^6. WASP-10 is a K dwarf with a spin period of 12 d and $J - K = 0.62$ and is rotating more slowly than stars of comparable colour in the Hyades (Terndrup et al. 2000). This suggests a rotational age between 600 Myr and 1 Gyr. Thus, the persistence of substantial orbital eccentricity in WASP-10b is therefore surprising.

One plausible mechanism for maintaining the high eccentricity is secular interaction with an additional planet in the system. Adams & Laughlin (2006) explore the effects of dynamical interactions among planets in extrasolar planetary systems and conclude that the outer planets can cause the inner planet to move through a range of eccentricities over time-scales that are short when compared to the lifetime of the system, but very long when compared to the current observational baseline. However, recently Matsumura, Takeda & Rasio (2008) have argued that an unseen companion driving short-period systems is unlikely. They present an upper limit of 1 $M_{\rm Neptune}$ for a possible unseen companion in the GJ 436 system and exclude this based on the current RV upper limits of $\leq$5 m s^{-1}. Matsumura et al. (2008) also present a range of tidal quality $Q_{\rm p}$ time-scales that could be as large as 10^9 yr, and argue that this new class of eccentric, short-period ESP is simply still in the process of circularizing. WASP-10b has not been extensively studied to rule out a putative outer plane that may be driving its eccentricity. Thus, the $\approx$6 per cent eccentricity of WASP-10b makes it an attractive target for future transit-timing variation studies, and for longer term RV monitoring to establish the mass and period of the putative outer planet.

The majority of transiting ESP found have masses below $1.5 M_J$, although there are a few more massive ESP. HD 17156 and COROT-Exo-2 have similar masses to WASP-10b and although there are two more massive ESP, the nearly 9 M_J HAT P-2 (HD 147506b) (Bakos et al. 2007) and 7.3 M_J WASP-14b (Joshi et al. 2008), this higher mass region has been poorly explored. Additional transiting objects in the mass range are important for completing the current ESP mass–radius relations and constraining their compositions. The current sample of transiting ESP reveals a large range of densities. We derive a mean density for WASP-10b of $\approx$1.89 g cm^{-3} (1.42 ρ_J) and it would lie along the higher density contour in a mass–radius plot (Pollacco et al. 2008; Sozzetti et al. 2007).

One ultimate goal of our transit-search programme is to provide the observational grist that will stimulate and advance refined models for the formation and evolution of the hot and very hot Jupiters (e.g. Burrows et al. 1997; Fortney, Marley & Barnes 2007; Seager et al. 2007). By thus constraining the underlying physics, we will have a richer context for the interpretation of the lower mass planets expected from missions such as COROT and Kepler.

ACKNOWLEDGMENTS

The SuperWASP Consortium consists of astronomers primarily from the Queen's University Belfast, St Andrews, Keele, Leicester, The Open University, Isaac Newton Group La Palma and Instituto de Astrofísica de Canarias. The SuperWASP Cameras were constructed and operated with funds made available from Consortium Universities and the UK's Science and Technology Facilities Council. SOPHIE observations have been funded by the Optical Infrared Coordination Network. The data from the Mercator and NOT telescopes were obtained under the auspices of the International Time of the Canary Islands. We extend our thanks to the staff of the ING and OHP for their continued support of SuperWASP-N and SOPHIE instruments. FPK is grateful to AWE Aldermaston for the award of a William Penney Fellowship.

REFERENCES

Adams F. C., Laughlin G., 2006, ApJ, 649, 992
Anderson D. R. et al., 2008, MNRAS, 387, 4
Bakos G. A. et al., 2007, ApJ, 670, 826
Blackwell D. E., Shallis M. J., 1977, MNRAS, 180, 177
Bouchy F., The Sophie Team, 2006, in Arnold L., Bouchy F., Moutou C., eds, Tenth Anniversary of 51 Peg-b: Status of and Prospects for Hot Jupiter Studies. Frontier Group, Paris, p. 319
Burrows A. et al., 1997, ApJ, 491, 856
Collier Cameron A. et al., 2007a, MNRAS, 380, 1230
Collier Cameron A. et al., 2007b, MNRAS, 375, 951
Fortney J. J., Marley M. S., Barnes J. W., 2007, ApJ, 659, 1661
Hebb L. et al.2008, A&A, submitted
Hellier C. et al.2008, ApJ, submitted (arXiv0805.2600)
Horne K. D., 2003, in Deming D. and Seager S., eds, ASP Conf. Ser. Vol. 294. Scientific Frontiers of Exoplanet Research. Astron. Soc. Pac., San Francisco, p. 361
Jackson B., Greenberg R., Barnes R., 2008, ApJ, 678, 1396
Joshi Y. C. et al.2008, MNRAS, submitted (arXiv0806.1478)
Mardling R. 2007, MNRAS, 382, 1768
Matsumura S., Takeda G., Rasio F. A., 2008, ApJ, 686, L29

Pollacco D. et al., 2006, PASP, 106, 1088
Pollacco D. et al., 2008, MNRAS, 385, 1576
Queloz D. et al., 2001, A&A, 379, 279
Seager S., Kuchner M., Hier-Majumder C. A., Militzer B., 2007, ApJ, 669, 1279
Smith A. M. S. et al., 2007, MNRAS, 373, 1151
Sozzetti A., Torres G., Charbonneau D., Latham D. W., Holman M. J., Winn J. N., Laird J. B., O'Donavan F. T., 2007, ApJ, 664, 1190
Stetson P., 1987, PASP, 99, 191
Stempels H. C., Collier Cameron A., Hebb L., Smalley B., Frandsen S., 2007, MNRAS, 379, 773
Terndrup D. M., Stauffer J. R., Pinsonneault M. H., Sills A., Yuan Y., Jones B. F., Fischer D., Krishnamurthi A., 2000, AJ, 119, 1303
Torres G., Konacki M., Sasselov D. D., Jha S., 2004, ApJ, 614, 979
Valenti J. A., Fischer D., 2005, ApJS, 159, 141
Valenti J. A., Piskunov N., 1996, A&AS, 118, 595
West R. et al.2008, A&A, submitted (arXiv0809.4597)
Wilson D. et al., 2008, ApJ, 675, 113

This paper has been typeset from a TEX/LATEX file prepared by the author.